

Super-k: A Piecewise Linear Classifier Based on Voronoi Tessellations

Rahman Salim Zengin^{a,c,1,*}, Volkan Sezer^{b,c,2}

^aDepartment of Mechatronics Engineering, Istanbul Technical University, Istanbul, Turkey

^bDepartment of Control and Automation Engineering, Istanbul Technical University, Istanbul, Turkey

^cAutonomous Mobility Group, Electrical and Electronics Engineering Faculty, Istanbul Technical University, Istanbul, Turkey

Abstract

Voronoi tessellations are used to partition the Euclidean space into polyhedral regions, which are called Voronoi cells. Labeling the Voronoi cells with the class information, we can map any classification problem into a Voronoi tessellation. In this way, the classification problem changes into a query of just finding the enclosing Voronoi cell. In order to accomplish this task, we have developed a new algorithm which generates a labeled Voronoi tessellation that partitions the training data into polyhedral regions and obtains interclass boundaries as an indirect result. It is called Supervised k-Voxels or in short Super-k. We are introducing Super-k as a foundational new algorithm and opening the possibility of a new family of algorithms. In this paper, it is shown via comparisons on certain datasets that the Super-k algorithm has the potential of providing comparable performance of the well-known SVM family of algorithms with less complexity.

Keywords: Supervised Learning, Piecewise Linear Classification, Voronoi Tessellations

1. Introduction

Piecewise Linear (PWL) classifiers are primitive and foundational types of classifiers. When limited computational resources are considered, they become appropriate tools for classification. To the best of our knowledge, almost all piecewise linear classifier literature focuses on hyperplanes, margins, and boundaries. It is very clear that these are critical concepts for the pattern classification. A detailed literature review about PWL classifiers can be found in[1].

Support Vector Machine (SVM)[2] was the most used classification algorithm before the deep learning revolution[3]. SVM had been constructed based on strong theoretical foundations. SVM obtains a separating hyperplane via choosing some of the training data instances, which are maximizing the margin, as support vectors. Although it is linear in the fundamental sense, with the help of kernel trick, the classification problem is translated into a higher order feature space, and nonlinear decision boundaries can be obtained for more complex classification problems. When the kernel trick is utilized, SVM still does its job as a linear classifier in that higher order feature space.

K-nearest neighbors (KNN)[4] is a nonparametric method of classification. Instead of obtaining a parametric model of the data, the data itself is used as the model. When a new sample arrives for classification, similar in-

stances of the training data are found based on a distance metric, mostly Euclidean distance. K-nearest training data instances constitutes a local distribution, around the prediction point. Using the labels of the k data instances, prediction can be done in many ways. Simple Bayesian statistics can be applied, as the labels can be weighted equally, or weighted according to the distances. Even a kernel function can be applied locally to determine the predicted label. A famous quote summarizes KNN in a nice way: "When I see a bird that walks like a duck and swims like a duck and quacks like a duck, I call that bird a duck." [5]

In this paper, a new machine learning algorithm, **Supervised k-Voxels** or in short **Super-k**, is introduced. The Super-k algorithm comprises several steps for processing the training data, and obtaining a classifier. Voxelization[6] is applied to classes of data separately, in order to obtain an initial Voronoi tessellation[7]. A simple variant of EM algorithm[8] is applied to distribute initial generator points over the data more uniformly. These steps result in separate Voronoi tessellations for different classes. Afterwards, the Super-k algorithm merges all separate class tessellations and labels the generator points, using the covered data via plurality voting. In the final phase, it applies a simple correction scheme to reduce False Positive (FP) classifications.

Due to the polyhedral shape of Voronoi cells, the Super-k algorithm is a PWL classification algorithm. Generator points, which are labeled using the class information, determine interclass boundaries. There is no direct consideration of hyperplanes or boundaries in the proposed approach. On the other hand, these hyperplanes and bound-

*Corresponding author

Email addresses: rszengin@itu.edu.tr (Rahman Salim Zengin), sezerv@itu.edu.tr (Volkan Sezer)

¹ORCID: <https://orcid.org/0000-0002-3104-4677>

²ORCID: <https://orcid.org/0000-0001-9658-2153>

aries are indirect results of Voronoi-based space partitioning.

As an enhancement, instead of Euclidean distance used in the definition of Voronoi tessellations, derived Super-k likelihood is used as a similarity metric. Maximization of the Super-k likelihood is equal to the minimization of Euclidean distance (A.5). Super-k likelihood has a computational performance advantage on modern hardware due to the matrix multiplication optimizations implemented in recent hardware platforms. It is applicable to any algorithm that relies on Euclidean distance for one-to-many comparisons.

The Super-k algorithm uses only simple arithmetic operations. Therefore, it can be implemented using only integer arithmetic for both training and inference. This enables the development of low-cost embedded platforms, not only for inference, but also for training.

It is possible to split a pretrained Super-k model into multiple classifiers. Similarly, separately trained Super-k models can be merged into a single model to obtain higher precision, or higher number of classes. On-line or hybrid learning scenarios can be implemented with this flexibility of the Super-k.

All alternate scenarios are left open and only the Super-k algorithm is explained in this paper. Following a short background information (Section 2), the Super-k algorithm is explained (Section 3). Afterwards, experimental results, classifications on synthetic data as well as comparisons against SVMs and KNN, are given (Section 4). Lastly, some ideas about possible improvements and applications of the Super-k algorithm are shared (Section 5).

2. Background

In this section, notations and some definitions used throughout this paper are provided.

2.1. Notation

Boldface denotes a vector and superscript T denotes transpose, such as $\mathbf{x} = (x_1, \dots, x_m)^T$.

The floor function is shown as $\lfloor \cdot \rfloor$, and $\lceil \cdot \rceil$ is the ceil function. Rounding to the nearest integer is shown as $\lceil \cdot \rceil$.

As piecewise linear (PWL) classification is done on multivariate data, Voronoi Tessellations[7] covering such data are defined in m dimensional Euclidean space, \mathbb{R}^m .

A Voronoi polyhedron is a convex region defined by an inner generator point and some outer generator points, as shown in (1).

$$V(\mathbf{p}_i) = \{\mathbf{x} \mid \|\mathbf{x} - \mathbf{p}_i\| \leq \|\mathbf{x} - \mathbf{p}_j\| \text{ for } j \neq i, i, j \in I_n = \{1, \dots, n\}\} \quad (1)$$

where $V(\mathbf{p}_i)$ denotes voronoi polyhedron with respect to the generator point \mathbf{p}_i .

The set of Voronoi polyhedra which creates the Voronoi tessellation is defined as $\mathcal{V} = \{V(\mathbf{p}_1), \dots, V(\mathbf{p}_n)\}$.

A generator point \mathbf{p}_i belongs to the set of generator points P of the Voronoi tessellation, hence, the set of generator points is $P = \{\mathbf{p}_1, \mathbf{p}_2, \dots, \mathbf{p}_n\}$.

Voronoi facets are sets of equidistant points between generator points as given in 2,

$$e_{ij} = \{\mathbf{x} \mid \|\mathbf{x} - \mathbf{p}_i\| = \|\mathbf{x} - \mathbf{p}_j\|\} \quad (2)$$

where $j \neq i$.

The whole set of facets of a Voronoi polyhedron is called a boundary and it is denoted related to the inner generator point of the region encircled as $\partial V(\mathbf{p}_i)$.

Labeling the generator points set P results in a labeled tessellation. Every Voronoi cell has a class designator ξ_i , which is defined with respect to \mathbf{p}_i . Set of all class designators of the generator points is defined as $\Xi = \{\xi_1, \dots, \xi_n\}$.

Superscript (t) denotes the value of a parameter for the iteration step of t .

In the classification plots, misclassified data instances are marked with red dots.

2.2. The Super-k Likelihood

If the logarithm of the multivariate normal distribution is simplified (Appendix A) for $\Sigma = I$ and equal priors are considered, for the maximum likelihood approximation, the derived likelihood function is given in (3).

$$g_i(\mathbf{x}) = \mathbf{x}^T \mathbf{p}_i - \frac{1}{2} \mathbf{p}_i^T \mathbf{p}_i \quad (3)$$

In order to understand the usage of (3), it can be separated into two parts as given in (4).

$$g_i(\mathbf{x}) = \underbrace{\mathbf{x}^T \mathbf{p}_i}_{\text{changing}} - \underbrace{\frac{1}{2} \mathbf{p}_i^T \mathbf{p}_i}_{\text{constant}} \quad (4)$$

After the training of a Super-k classifier, the generator points become constant. Then, the second part of (4) is composed of just constant numbers, and computing them at once for a trained model is enough. Hence, the computation of the Super-k likelihood is a reduction to the inner product of two vectors, plus a constant. The computation of the Super-k likelihood can be done with a single *Basic Linear Algebra Subprograms* (BLAS)[9] Level 1 function call. Almost every modern hardware platform has vector computation capabilities which makes them very suitable for the acceleration.

3. The Super-k Algorithm

In order to convert the training data to a Voronoi Tessellation-based representation, the spaces, which are covering the whole range of every class of the data, are divided into voxels separately per every class. Instances of the training data are partitioned into voxelized subsamples through this process. Some of the voxels might be empty, some others might include varying numbers of instances.

For every nonempty voxel, the mean of the included instances is calculated. These voxel means create the initial tessellation of the class and represent the generator points of the class.

Tessellating the data through a uniform voxelization process might result in a nonideal tessellation, and possibly creates degenerate³ Voronoi vertices. The generator points and class data are passed through a simple Expectation-Maximization process to evenly distribute the generator points over the class instances. In this way, possible degenerate Voronoi vertices are removed, and the generator points move closer to the centroids of the Voronoi cells.

All separately created Voronoi tessellations are merged into a single tessellation via combining the generator points of every class. When all the generators are combined within some overlapping regions between classes, some of the generator points might become minorities, compared to the enclosed data instances. In order to make sure that all of the generator points represent the assigned instances correctly, labeling via plurality voting is performed.

Finally, with the goal of reducing FP classifications, a correction is applied to the generator points via excluding FP instances from the relevant Voronoi cells. This correction reduces the classification error without causing overfitting of the training data.

The main steps of the Super-k algorithm is shown in (Figure 1)). Each of these steps are explained in detail, in the following sections.

3.1. Multidimensional Voxelization

Voxelization of multidimensional data is not as simple as doing so with 3-D data. Dividing the space, covered with the whole range of data using all dimensions might create impractically a high number of voxels. For \mathbb{R}^m , if every dimension is divided into b ranges, the number of total voxels would be b^m . For a sample size of N , there can be at most N nonempty voxels. However, having just one data instance in every nonempty voxel merely gives back the original data, after the voxelization process. For a meaningful voxelization, some of the nonempty voxels must have multiple data instances. Therefore, the number of nonempty voxels must be less than the sample size N . Thus, when a uniformly distributed data is considered, the practicability condition of voxelization can be defined as $b^m < N$ or via taking the logarithm of both sides with respect to b , it becomes $m < \log_b N$.

In order to accomplish the task of voxelization of multidimensional data, an empirical method is developed. k is an indirect parameter which specifies the minimum number of required voxels. It is not a precision parameter and its effect depends on the data. Multiple values of k might give the same result. In order to understand the reasoning behind our assumptions, a numerical example will be provided. Afterwards, relevant equations will be given.

³For the degenerate cases see page 46 of [7]

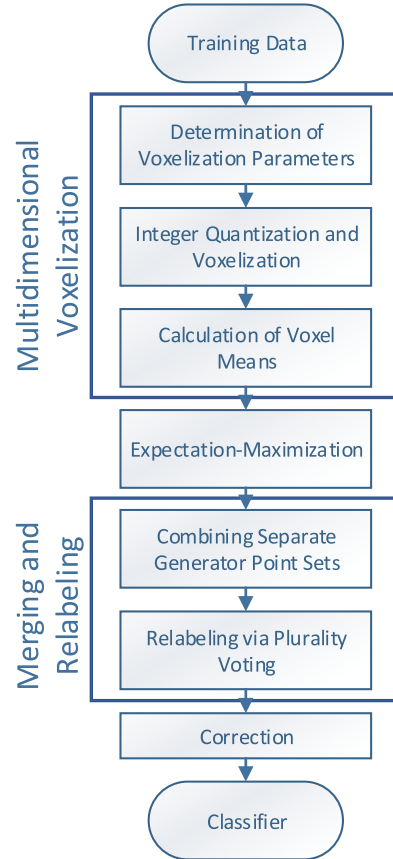


Figure 1: The Super-k algorithm processing steps

Let us assume that for a given dataset, the sample size of the data is $N = 1000$, the dimensionality of the data is $m = 100$, and the requested number of voxels is $k = 50$. We need to calculate b in order to find how many divisions are required for each axes. The value of b can only be an integer. Thus, let us define another real number parameter c , the scale of divisions, and relate it to b as $b = \lceil c \rceil$. From the definition of k , we can write $c^m = k$ and obtain c using k as $c = \sqrt[m]{k}$. Using the numerical values provided in the example, the value of c can be found as $c = \sqrt[100]{50} = 1.039896$. It is not possible to divide the dimensions into fractional ranges, hence, this number is not usable. If we round this number to the next higher integer value, b is found as $b = \lceil c \rceil = 2$. This value of b is usable for the voxelization. However, now, the number of voxels becomes $b^m = 2^{100} = 1267650600228229401496703205376$. This number is higher than all the memories in the world.

If we use not all, but a small subset of the dimensions for the voxelization, it will be possible to obtain a more reasonable number of voxels. Let us designate the number of dimensions to use as m_v , which we name as the number of variant features. Furthermore, let us introduce another parameter, $a = \lfloor c \rfloor$, which we use for the number of divisions of the unselected dimensions. Relation of b with c is $b = \lceil c \rceil$. With these definitions, our aim is to approximate c with the integers a and b , such that, $a^{(m-m_v)}b^{m_v} \approx c^m$.

Then, m_v can be given as,

$$m_v = \left\lceil m \frac{\log\left(\frac{c}{a}\right)}{\log\left(\frac{b}{a}\right)} \right\rceil \quad (5)$$

Derivation of (5) can be found in (Appendix B).

For our numerical example, when we do the calculations using (5), the result becomes $m_v = \lceil 5.643856 \rceil = 6$.

The selection of the variant features is another critical issue. Although the variance shows spread of data, it cannot measure how uniformly the data spreads over the existing values. Under these considerations, the number of unique values for every feature is used as a measure for the selection of the variant features. The higher the number of the unique values is, the better it makes the voxelization.

The final step of the voxelization is the determination of the same voxel instances via quantization and voxel means calculation. Min to max ranges of the data is divided into the number of steps, separately for every data feature. Using this resolution parameter, the whole data is converted to integer indices, which designate the voxel indices of the data instances. Then, the means of all nonempty voxels are calculated using the instances inside. The related pseudocode is given in (Algorithm 1). The voxelization process is also illustrated in (Figure 2), where voxelization of two classes is shown separately. For $k = 5$, the algorithm determines 3×2 partitioning of the whole range for both classes. For class 0 (Figure 2a), there are 5 nonempty voxels. For class 1 (Figure 2a), the number of nonempty voxels is 4. Data instances in separate voxels are shown in different colors. The voxel means are also shown as cyan circles with voxel indices inside. These two separate results can be seen combined in (Figure 3a).

Function Voxelize(k)

Data:

$X \leftarrow [\mathbf{x}_1 \ \dots \ \mathbf{x}_N]$ /* Instances */

Result: $Means$ /* Voxel means */

begin

$c = \sqrt[k]{m}$; $a = \lfloor c \rfloor$ $b = \lceil c \rceil$

$$m_v = \left\lceil m \frac{\log\left(\frac{c}{a}\right)}{\log\left(\frac{b}{a}\right)} \right\rceil$$

for $i = 1, \dots, m$ **do** /* every dimension */

 | $Counts[i] \leftarrow \text{CountUniqueValues}$

end

/* Get indices of m_v maximum */

$DimIndices \leftarrow \text{ArgK-Max}(Counts, m_v)$

$X_v \leftarrow \text{GetDims}(X, DimIndices)$

/* Quantize over selected dimensions */

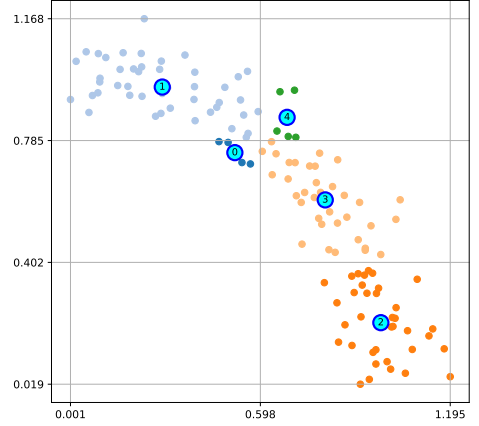
$Indices \leftarrow \text{Quantize}(X_v)$

/* Map voxel indices back to the data
and calculate voxel means */

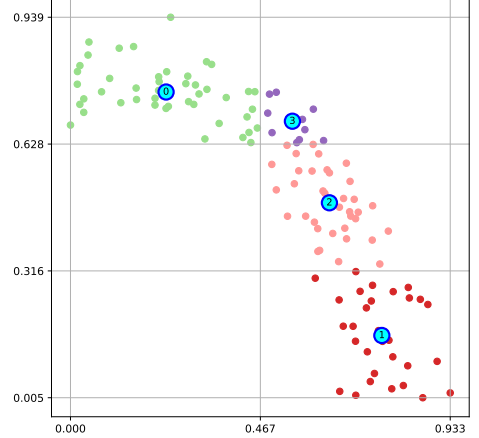
$Means \leftarrow \text{CalculateMeans}(X, Indices)$

end

Algorithm 1: Multidimensional Voxelization

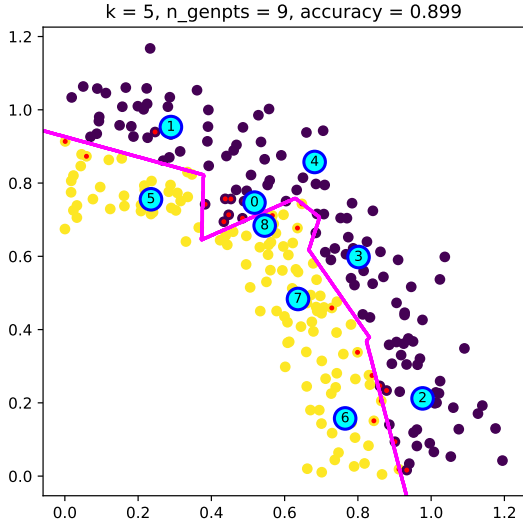


(a) Class 0

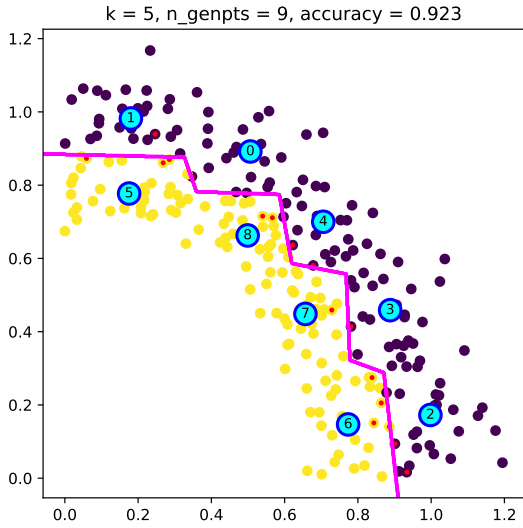


(b) Class 1

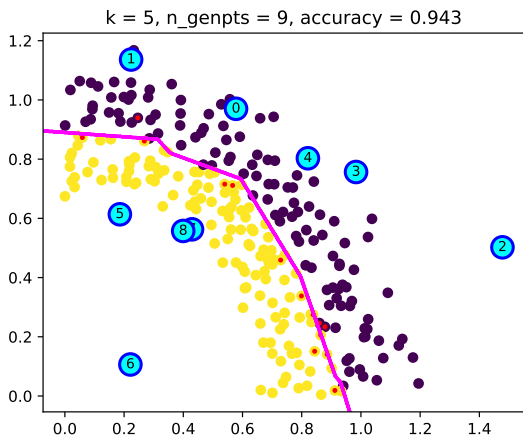
Figure 2: Voxelization grids, voxel members, and voxel means



(a) Voxelization



(b) EM



(c) Correction

Figure 3: Training steps of the Super-k algorithm

3.2. Cycling Through EM

A very simple variant of the Expectation-Maximization (EM) algorithm is used to distribute generator points over the class instances, more uniformly.

The Super-k likelihood (3) is used for the maximization step. The expectation step is the calculation of the means of the instances assigned to the same generator points. The effect of applying EM can be seen if (Figure 3a) is compared with (Figure 3b). The generator point 0 moves up, and the generator points 4 and 3 move downright. As a result, the accuracy of the classification is improved from 89.9% to 92.3% at the end of this step, as shown in (Figure 3). Pseudocode of the EM variant is given in (Algorithm 2).

Function ApplyEM(n_{cycles})

Data:

$X \leftarrow [x_1 \ \dots \ x_N]$ /* Instances */

$P \leftarrow [p_1 \ \dots \ p_n]$ /* Generator Points */

Result: P : /* Generator Points */

begin

for $i = 1, \dots, n_{cycles}$ **do**

 /* Assign data instances to the generator points */

$Assignments \leftarrow \text{Argmax}(\text{Likelihood}(X, P))$

 /* Recalculate generator points from the assigned instances */

foreach p_i **in** P **do**

$p_i \leftarrow \text{Mean}(X[Assignments = i])$

end

end

end

Algorithm 2: Simple EM variant

3.3. Merging and Relabeling

In order to create a single Voronoi tessellation from separately created class tessellations, all generator points should be merged and labeled according to the pluralities of the data instances covered. The merging of two separate classes can be understood via examination of (Figure 2) and (Figure 3a). The difference of plurality voting from majority voting is that plurality has the highest number of votes but might be less than half of all votes, while majority takes more than half of all votes. When multiple classes are considered, plurality voting is more suitable. Related pseudocode is given in (Algorithm 3).

3.4. Correction

Every Voronoi cell is defined by its generator point. Due to the labeling of the generator points, some of the data instances in the relevant Voronoi cell, might belong to another class. Therefore, these instances are the FPs of that Voronoi cell. If these FP instances are close to the cell boundary, moving the generator point away from the FP

```

Function MergeAndRelabel( $n_{classes}$ )
Data:
 $X \leftarrow [x_1 \ \dots \ x_N]$  /* Instances */
 $y \leftarrow [y_1 \ \dots \ y_N]$  /* Labels */
/*  $\mathcal{P}$ : Set of Class Generators */
 $\mathcal{P} \leftarrow \{P_1, \dots, P_{n_{classes}}\}$ 
Result:
 $P$ : /* Combined Generator Points */
 $\Xi$ : /* Generator Point Labels */
begin
   $P \leftarrow \text{Combine}(\mathcal{P})$ 
  /* Assign data instances to the
     generator points */
   $Assn = \text{Argmax}(\text{Likelihood}(X, P))$ 
  foreach  $p_i$  in  $P$  do
    |  $Counts \leftarrow \text{CountUnique}(y[Assn = i])$ 
    |  $\xi_i \leftarrow \text{Argmax}(Counts)$ 
  end
end

```

Algorithm 3: Merging and Labeling of the combined tessellation

instances will leave them out of the Voronoi cell. In order to apply this simple correction idea, the generator points are weighted with the number of all assigned instances and the FP instances are subtracted from the generator points. Repetitive application of this correction (6) improves classification accuracy without causing overfitting. An example result of correction is shown in (Figure 3c). If it is compared with the uncorrected state (Figure 3b), change of the decision boundary is apparent. The generator points move away from the boundary, and the boundary becomes smoother. As a result, the accuracy is improved from 92.3% to 94.3% for the provided example.

$$\mathbf{p}_i^{(t+1)} = \frac{\mathbf{p}_i^{(t)} * n_{all} - \sum \mathbf{x}_{FP}}{n_{all} - n_{FP}} \quad (6)$$

The pseudocode of the correction procedure is given in (Algorithm 4).

3.5. Classification with Super-k

Classification using the trained Super-k model is the maximization of the Super-k likelihood over i (7). This maximization is straightforward to implement with a few lines of code. When (7) is applied, the class label of the i 'th generator point becomes the classification result. The advantage of the Super-k likelihood is mentioned in (Section 2.2). Its relation to the Euclidean distance is explained in (Appendix A).

$$\xi(x) = \underset{i}{\operatorname{argmax}} \left(\mathbf{x}^T \mathbf{p}_i - \frac{1}{2} \mathbf{p}_i^T \mathbf{p}_i \right) \quad (7)$$

```

Function Correction( $n_{cycles}$ )
Data:
 $X \leftarrow [x_1 \ \dots \ x_N]$  /* Instances */
 $P \leftarrow [p_1 \ \dots \ p_n]$  /* Generator Points */
Result:  $P_{best}$ : /* Generator Points */
begin
   $best\_accuracy = 0$ 
  for  $i = 1, \dots, n_{cycles}$  do
    | foreach  $p_i$  in  $P$  do
    | |  $p_i = (p_i * n_{all} - \sum \mathbf{x}_{FP}) / (n_{all} - n_{FP})$ 
    | end
    | /* Keep best params */
    | if  $accuracy > best\_accuracy$  then
    | |  $best\_accuracy = accuracy$ 
    | |  $P_{best} = P$ 
    | end
  end
end

```

Algorithm 4: Correction

4. Experimental Results

The platform used for the experimental tests and comparisons is as follows: The CPU used for the experimentation is Intel(R) Core(TM) i7-7700 running at 3.60GHz frequency; the system has 32GB of DDR4 RAM running at 2133 MHz.

SVM and KNN are inherently PWL classifiers. SVM chooses some near the boundary data instances. KNN creates Voronoi-like partitioning. Classification with Super-k is similar to 1-NN classification. Due to such similarities, the Super-k algorithm is compared against these algorithms.

Unoptimized reference implementation of the Super-k algorithm is written in Python[10] using the related libraries[11, 12]. Scikit-Learn[13] is used for both synthetic data generation and dataset retrieval. In addition, the SVM variants and KNN are used from the same library[13]. According to the library documentation, for Linear-SVM, LibLinear[14] is used in the background. Besides, LibSVM is used for the kernel based SVMs by the library.

The reference implementation of the Super-k algorithm and the source code to reproduce the results of this paper are shared[15].

4.1. Tests with synthetic datasets

The Super-k algorithm is tested on synthetic datasets especially for visualization purposes. Using the library tools, 2 class moons (Figure 4), 2 class circles (Figure 5) and 3 class random gaussians (Figure 6) are generated. All datasets are processed using different values of k. The instances of different classes are shown in distinctive colors. The misclassified instances are marked with red dots. The generator points are shown as cyan circles with the

generator point index numbers inside. The boundaries between the generator points of different classes are shown in magenta.

The Super-k algorithm creates PWL boundaries between different classes of data. It can be seen on figures that increasing the number of generator points increases the detail of the decision boundaries. On the other hand, the increase in the detail does not always mean significantly better classification accuracy. On the moons dataset (Figure 4), the accuracies for different k values are almost the same.

When the generator points from different classes come closer, their relative orientation becomes more important. On the circles dataset (Figure 5), sawtooth-like structures with sharp corners occur on the decision boundary. For the low number of the generator points, such shapes might become bigger and increase the classification error. During the development of super-k algorithm, such drawbacks and possible precautions are ignored for the sake of simplicity of the algorithm. With increasing k , such artifacts become less effective and the total error decreases.

The obtained generator points do not necessarily occur on the data. This phenomenon can be identified clearly on (Figure 6a). The generator point 5 is placed out of the data, but in competition with the generator point 3, it defines the boundary between the yellow and green colored regions.

4.2. Tests with real world datasets

In this study, the SVM family of algorithms are used for comparison. Additionally, KNN is used as another reference method. The SVM variants[14, 16] used for the comparisons are linear SVM (Linear SVM), SVM with Linear kernel (SVM Linear), SVM with RBF kernel (SVM RBF), and SVM with polynomial kernel (SVM Poly). Five real world datasets[17] (Table 1a) are selected for testing. Both the training (Table 1c) and test (Table 1d) runs are repeated for 10 times. In order to reduce the OS scheduler related timing noise, every run is continued at least 1 seconds. The provided results are the mean values of the durations and the standard deviations in parentheses. Certain parameters of the algorithms are determined via 5-fold cross validation (CV), for every dataset separately. Because the CV process takes long, determined parameters are saved for later reuse.

As it can be seen from the accuracies (Table 1b), the Super-k algorithm produces results that are similar to the other algorithms.

When training times (Table 1c) are considered, the Super-k algorithm has comparable performance with the SVM family of algorithms.

Similarly, when we compare the inference performance of the algorithms (Table 1d), performance of Super-k is comparable with linear SVM, and is better than the others.

5. Conclusion

A new foundational PWL classification algorithm, **Super-k**, which is inspired from well known ideas, is introduced in this paper. The contributions of the proposed algorithm are as follows:

- A method for voxelization of multidimensional data is proposed.
- A simple and efficient likelihood function is introduced, and under some conditions, its usage in place of Euclidean distance is explained.
- A new approach for data classification, based on Voronoi tessellations, is presented.

Super-k might help the applications that have a limited computational resource. Space systems have limited onboard resources and restrictions on the power budget. For such systems, SVM is considered[18, 19] as a solution. The Super-k algorithm might be an alternative for such requirements.

The proposed algorithm can be improved in many ways and the ideas that created the Super-k algorithm may open ways to many different solutions.

Acknowledgements

This research was supported by the Turkish Scientific and Technological Research Council (TUBITAK) under project no. 118E809.

We would like to thank the reviewers for their thoughtful comments and their constructive remarks.

Appendix A. Derivation of Super-k Likelihood

The Super-k likelihood function (3) can be derived from the logarithm of multivariate normal distribution (A.1).

$$p(x|\omega) = \frac{1}{(2\pi)^{\frac{d}{2}}|\Sigma|^{\frac{1}{2}}} \exp\left[-\frac{1}{2}(x-\mu)^T\Sigma^{-1}(x-\mu)\right] \quad (\text{A.1})$$

$$g_i(x) = \ln p(x|\omega_i)$$

$$= -\frac{1}{2}(x-\mu_i)^T\Sigma^{-1}(x-\mu_i) - \frac{d}{2}\ln(2\pi) - \frac{1}{2}\ln|\Sigma| \quad (\text{A.2})$$

Expanding (A.2) and making $\Sigma = I$ gives

$$g_i(x) = -\frac{1}{2}[x^T x - x^T \mu_i - \mu_i^T x + \mu_i^T \mu_i] - \frac{d}{2}\ln(2\pi) \quad (\text{A.3})$$

For a two-side comparison between $g_i(x)$ and $g_j(x)$, the constant terms have no effect. Removing the terms in (A.3), the constant with respect to i gives

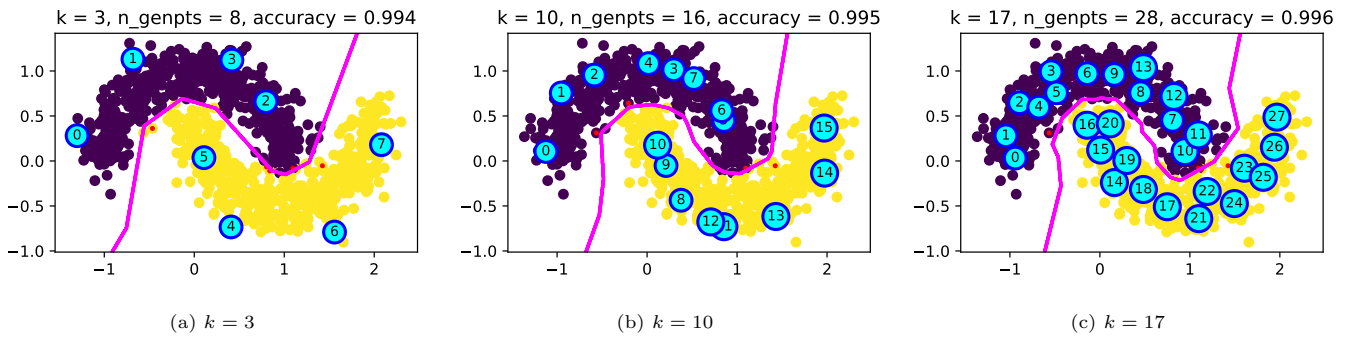


Figure 4: Test results on synthetic moons dataset

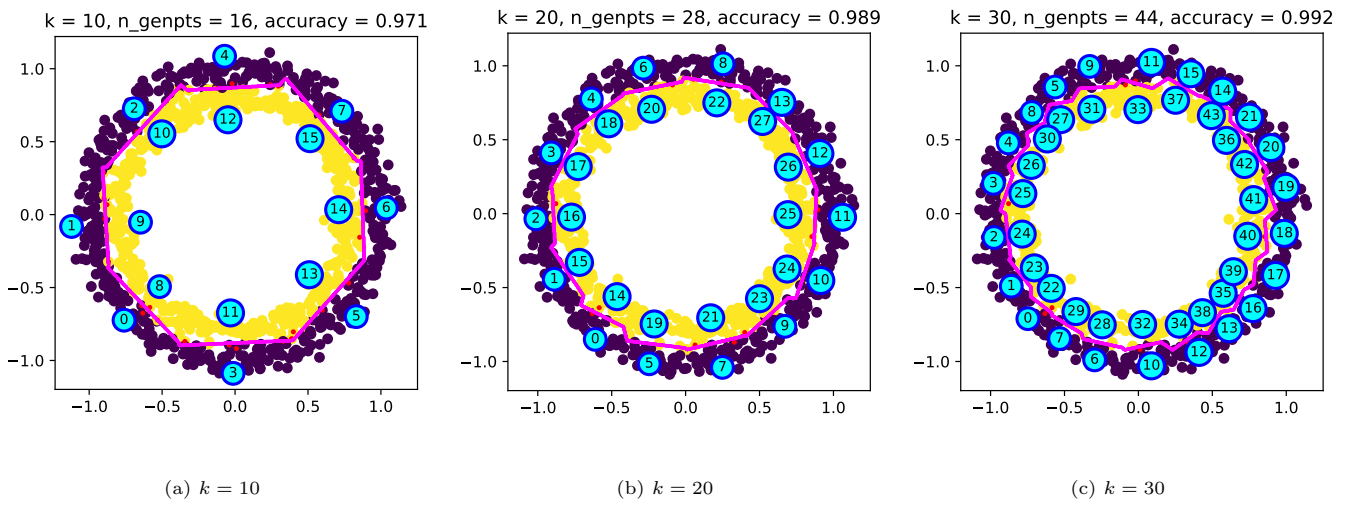


Figure 5: Test results on synthetic circles dataset

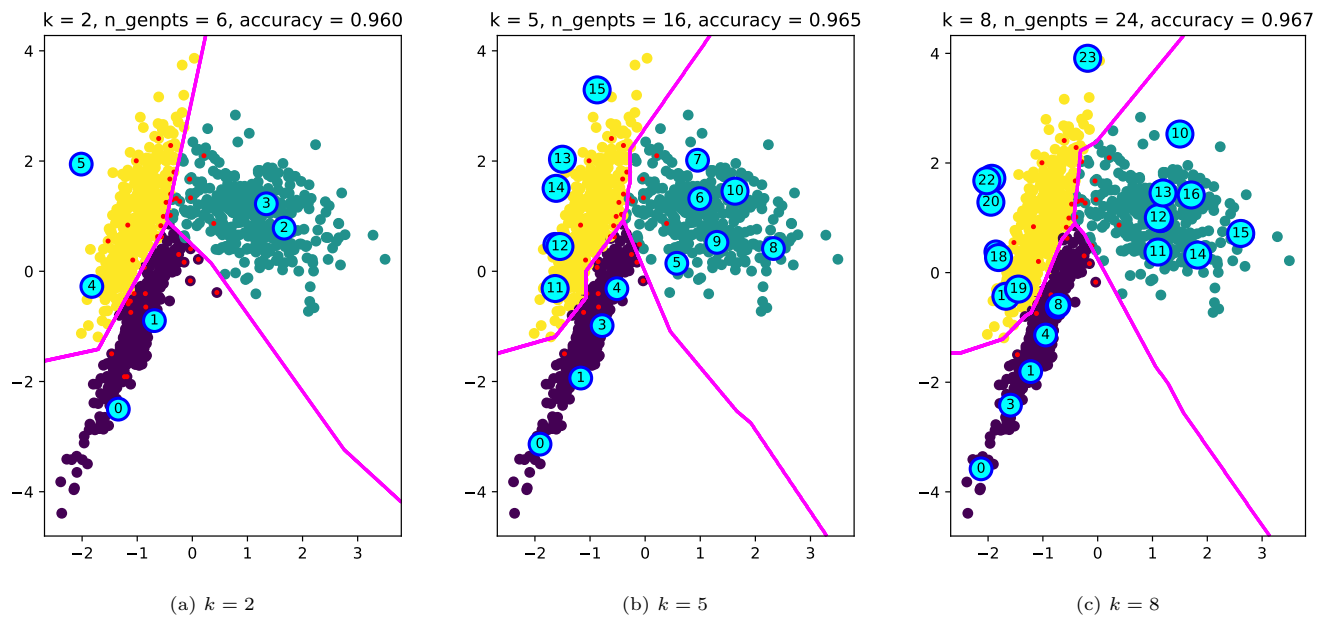


Figure 6: Tests results on randomly generated gaussians

Table 1: Experimental results with real world datasets

(a) Datasets

	Sample Size	Features	Train/Test Sizes
optdigits	5620	64	3823/1797
USPS	9298	256	7291/2007
satimage	6430	36	5144/1286
letter	20000	16	16000/4000
isolet	7797	617	6240/1557

(b) Test accuracies

	optdigits	USPS	satimage	letter	isolet
Super-k	0.976	0.943	0.918	0.950	0.940
Linear SVM	0.950	0.915	0.835	0.701	0.956
SVM Linear	0.962	0.935	0.877	0.850	0.959
SVM RBF	0.983	0.954	0.918	0.979	0.969
SVM Poly	0.975	0.951	0.896	0.955	0.969
KNN	0.980	0.950	0.911	0.961	0.927

(c) Training times in milliseconds, Mean(StdDev)

	optdigits	USPS	satimage	letter	isolet
Super-k	1008.9(16.1)	5651.8(232.0)	285.1(37.7)	3534.4(1769.6)	1628.0(148.3)
Linear SVM	96.2(3.9)	1670.4(78.0)	126.0(6.4)	1580.2(104.5)	6061.3(50.7)
SVM Linear	139.5(11.5)	1477.2(93.3)	361.7(24.3)	3784.7(163.3)	5525.9(142.1)
SVM RBF	387.6(18.6)	2230.2(137.9)	504.1(8.2)	15299.6(834.5)	12867.2(245.0)
SVM Poly	129.6(1.2)	1773.6(213.2)	421.5(11.3)	2649.8(30.2)	7824.1(123.2)
KNN	19.2(1.4)	165.7(5.6)	17.1(0.8)	52.5(0.7)	266.0(3.1)

(d) Inference times in milliseconds, Mean(StdDev)

	optdigits	USPS	satimage	letter	isolet
Super-k	3.4(0.2)	12.1(0.8)	0.8(0.1)	34.1(13.7)	2.4(0.3)
Linear SVM	1.8(0.2)	2.1(0.2)	1.1(0.0)	3.8(0.3)	2.8(0.3)
SVM Linear	67.9(3.1)	644.2(35.2)	81.3(2.2)	1138.9(37.9)	4177.0(219.8)
SVM RBF	183.1(3.5)	903.4(80.6)	135.4(4.6)	2523.8(188.6)	5312.9(218.9)
SVM Poly	102.6(12.4)	946.0(75.0)	78.5(2.5)	793.7(65.4)	4137.8(253.8)
KNN	290.5(61.3)	1380.8(388.0)	146.4(3.9)	338.9(22.6)	3443.5(1559.9)

$$\begin{aligned}
g_i(x) &= -\frac{1}{2} [-x^T \mu_i - \mu_i^T x + \mu_i^T \mu_i] \\
g_i(x) &= x^T \mu_i - \frac{1}{2} \mu_i^T \mu_i
\end{aligned} \tag{A.4}$$

As a result of such simplifications, the Super-k likelihood (A.4) has been obtained.

When one-to-many comparisons are considered, it can be shown that maximizing the super-k likelihood is the same as minimizing the Euclidean distance.

$$\operatorname{argmax}_i \left(\mathbf{x}^T \mathbf{p}_i - \frac{1}{2} \mathbf{p}_i^T \mathbf{p}_i \right) = \operatorname{argmin}_i (\|\mathbf{x} - \mathbf{p}_i\|) \tag{A.5}$$

When the right hand side of (A.5) is expanded,

$$\begin{aligned}
&\operatorname{argmin}_i (\|\mathbf{x} - \mathbf{p}_i\|) \\
&= \operatorname{argmin}_i \sqrt{(\mathbf{x} - \mathbf{p}_i)^T (\mathbf{x} - \mathbf{p}_i)} \\
&= \operatorname{argmin}_i \sqrt{\mathbf{x}^T \mathbf{x} - \mathbf{x}^T \mathbf{p}_i - \mathbf{p}_i^T \mathbf{x} + \mathbf{p}_i^T \mathbf{p}_i}
\end{aligned} \tag{A.6}$$

The square root operation is a monotonic function, hence, removing it does not affect the ordering. Also $\mathbf{x}^T \mathbf{x}$ in (A.6) is a constant with respect to i , thus it is the same on both sides of the comparisons and can be removed.

$$\operatorname{argmin}_i (\|\mathbf{x} - \mathbf{p}_i\|) = \operatorname{argmin}_i (-2\mathbf{x}^T \mathbf{p}_i + \mathbf{p}_i^T \mathbf{p}_i) \tag{A.7}$$

Multiplying (A.7) with $-\frac{1}{2}$ only changes the direction of the ordering, hence, argmin becomes argmax (A.8).

$$\operatorname{argmin}_i (\|\mathbf{x} - \mathbf{p}_i\|) = \operatorname{argmax}_i \left(\mathbf{x}^T \mathbf{p}_i - \frac{1}{2} \mathbf{p}_i^T \mathbf{p}_i \right) \tag{A.8}$$

Appendix B. Derivation of m_v

Our aim is to approximate k , using only integer values. We define a parameter c such that $c^m = k$. Most of the time, the value of c is not an integer. But it is possible to define lower and upper integer bounds for c , such that $a \leq c \leq b$, where a, b are integer values. It is possible to calculate c , such that $c = \sqrt[m]{k}$. Then, a and b can be found as $a = \lfloor c \rfloor$ and $b = \lceil c \rceil$.

The exponent is a monotonic function for positive real numbers. We know that c must be in somewhere between a and b . Thus, taking the exponent of the bounds, $a^m \leq c^m \leq b^m$ must be also true. Then, there must be a value of m_v that satisfies the condition $a^{(m-m_v)} b^{m_v} = c^m$. If we restrict m_v to be an integer, the condition can only be an approximation. Using that approximation, we can derive an equation (B.1) for the approximate integer value of m_v .

$$\begin{aligned}
a^{(m-m_v)} b^{m_v} &\approx c^m \\
a^m a^{-m_v} b^{m_v} &\approx c^m \\
\left(\frac{b}{a}\right)^{m_v} &\approx \left(\frac{c}{a}\right)^m \\
m_v &\approx m \frac{\log\left(\frac{c}{a}\right)}{\log\left(\frac{b}{a}\right)}
\end{aligned} \tag{B.1}$$

If we round the right hand side of (B.1) to the nearest integer, the equation for finding m_v (B.2) becomes

$$m_v = \left\lceil m \frac{\log\left(\frac{c}{a}\right)}{\log\left(\frac{b}{a}\right)} \right\rceil \tag{B.2}$$

which is the number of variant features.

References

- [1] Q. Leng, Z. He, Y. Liu, Y. Qin, Y. Li, A soft-margin convex polyhedron classifier for nonlinear task with noise tolerance, *Applied Intelligence* (Aug. 2020). doi:10.1007/s10489-020-01854-6.
- [2] C. Cortes, V. Vapnik, Support-Vector Networks, *Machine Learning* 20 (3) (1995) 273–297. doi:10.1023/A:1022627411411.
- [3] V. Carletti, A. Greco, G. Percannella, M. Vento, Age from Faces in the Deep Learning Revolution, *IEEE Transactions on Pattern Analysis and Machine Intelligence* 42 (9) (2020) 2113–2132. doi:10.1109/TPAMI.2019.2910522.
- [4] R. O. Duda, P. E. Hart, D. G. Stork, *Pattern Classification*, 2nd Edition, John Wiley & Sons, 2000.
- [5] J. W. Riley, James Whitcomb Riley - Poems & Prose Sketches: "When I See a Bird That Walks like a Duck and Swims like a Duck and Quacks like a Duck, I Call That Bird a Duck.", 2017.
- [6] T. Hinks, H. Carr, L. Truong-Hong, D. F. Laefer, Point Cloud Data Conversion into Solid Models via Point-Based Voxelization, *Journal of Surveying Engineering* 139 (2) (2013) 72–83. doi:10.1061/(ASCE)SU.1943-5428.0000097.
- [7] A. Okabe, *Spatial Tessellations: Concepts and Applications of Voronoi Diagrams*, 2nd Edition, Wiley Series in Probability and Statistics, Wiley, Chichester ; New York, 2000.
- [8] R. M. Neal, G. E. Hinton, A View of the Em Algorithm that Justifies Incremental, Sparse, and other Variants, in: M. I. Jordan (Ed.), *Learning in Graphical Models*, NATO ASI Series, Springer Netherlands, Dordrecht, 1998, pp. 355–368. doi:10.1007/978-94-011-5014-9_12.
- [9] S. Blackford, Quick Reference Guide to the BLAS, <https://www.netlib.org/lapack/lug/node145.html> (1999).
- [10] G. van Rossum, Python tutorial, technical report CS-R9526, centrum voor wiskunde en informatica (CWI), amsterdam." (1995).
- [11] S. van der Walt, S. C. Colbert, G. Varoquaux, The NumPy Array: A Structure for Efficient Numerical Computation, *Computing in Science Engineering* 13 (2) (2011) 22–30. doi:10.1109/MCSE.2011.37.
- [12] J. D. Hunter, Matplotlib: A 2D Graphics Environment, *Computing in Science Engineering* 9 (3) (2007) 90–95. doi:10.1109/MCSE.2007.55.
- [13] F. Pedregosa, G. Varoquaux, A. Gramfort, V. Michel, B. Thirion, O. Grisel, M. Blondel, P. Prettenhofer, R. Weiss, V. Dubourg, J. Vanderplas, A. Passos, D. Cournapeau, M. Brucher, M. Perrot, E. Duchesnay, Scikit-learn: Machine learning in Python, *Journal of Machine Learning Research* 12 (2011) 2825–2830.
- [14] R.-E. Fan, K.-W. Chang, C.-J. Hsieh, X.-R. Wang, C.-J. Lin, LIBLINEAR: A Library for Large Linear Classification, *The Journal of Machine Learning Research* 9 (2008) 1871–1874.
- [15] R. S. Zengin, V. Sezer, Ituamg/super-k: 2021.06, Zenodo (Jun. 2021). doi:10.5281/zenodo.4939965.
- [16] C.-C. Chang, C.-J. Lin, LIBSVM: A library for support vector machines, *ACM Transactions on Intelligent Systems and Technology* 2 (3) (2011) 27:1–27:27. doi:10.1145/1961189.1961199.
- [17] J. Vanschoren, J. N. van Rijn, B. Bischl, L. Torgo, OpenML: Networked science in machine learning, *SIGKDD Explorations* 15 (2) (2013) 49–60. doi:10.1145/2641190.2641198.
- [18] C. Shang, D. Barnes, Fuzzy-rough feature selection aided support vector machines for Mars image classification, *Computer Vision and Image Understanding* 117 (3) (2013) 202–213. doi:10.1016/j.cviu.2012.12.002.
- [19] A. M. Jallad, L. B. Mohammed, Hardware Support Vector Machine (SVM) for satellite on-board applications, in: 2014 NASA/ESA Conference on Adaptive Hardware and Systems (AHS), 2014, pp. 256–261. doi:10.1109/AHS.2014.6880185.